Check for updates

Reactivity of oxidized polonium towards quartz and α-Al2O3 surfaces

Katharina Hermainski, [ID] *[a] Alexander Yakushev, [ID] [b] Dominik Dietzel, [ID] [ab]
Christoph Emanuel Düllmann, [ID] [abc] Jochen Ballof, [ID] [b] Pavol Mošat', [ID] [b]
Felix Sprunk, [ID] [ab] Maxim Saifulin, [ID] [b] Pavel Bartl, [ID] [d] Jan John, [ID] [d]
Mojmír Němec, [ID] [d] Jon Petter Omtvedt, [ID] [e] Jan Štursa [ID] [f] and Václav Zach [ID] [f]

The chemistry of the radioelement polonium has attracted increasing attention owing to its formation in accelerator-driven systems and its high radiotoxicity. Being the lighter homologue of the superheavy element livermorium, whose chemistry is still unexplored, studies of polonium provide a benchmark for verifying the structure of the periodic table at the heavy-element frontier. While the reactivity of elemental polonium towards various surfaces in inert or reducing atmospheres has been investigated previously, the reactivity of oxidized polonium towards quartz has not been explored in detail. Here, we report on gas–solid thermochromatography studies of polonium on quartz glass and α-Al2O3 surfaces in helium, as well as in oxygen- and water-containing atmospheres in the atom-at-a-time regime. We found that polonium chemically reacts in an oxygen-containing atmosphere, forming two oxidized species, which are less volatile than elemental polonium. The chemical reaction is influenced by the water vapour concentration in the carrier gas and the applied temperature. The adsorption enthalpy of elemental polonium on α-Al2O3 in pure helium gas was determined to be -85^{+4}_{-3} kJ mol^{-1}, which is identical to the adsorption enthalpy on quartz as reported earlier. The results of the reported measurements will support future experiments with the superheavy element livermorium.

Introduction

Many previous studies of polonium have focused on the impact of the element's high radiotoxicity on the environment.[1,2] However, understanding the gas phase chemistry of polonium is also becoming increasingly important due to the development of accelerator-driven systems, which aim for the transmutation of long-lived, radiotoxic actinides in spent nuclear fuel.[3] During operation of such systems, polonium is produced by the interaction of protons or neutrons with bismuth, which is used in the form of lead–bismuth eutectic as a reactor coolant or spallation target. Thus, to ensure the safe operation of such systems, understanding the behaviour of polonium in a gaseous environment is vital.[4–6]

In addition, polonium, as the lighter homologue of livermorium (element 116), is now gaining increasing interest in the field of superheavy element (SHE) studies. The study of SHEs provides valuable insights into the influence of relativistic effects on chemistry.[7] As these effects scale approximately with the square of the atomic number, the study of SHEs is particularly suitable to better understand the fundamental influence of relativistic effects on all elements of the periodic table.[8] The heaviest SHE chemically investigated to date is moscovium (element 115).[9] Thus, the focus now shifts to the next heavier element, livermorium. The investigation of polonium is a first step towards exploring the chemistry of the element livermorium.

A higher chemical reactivity is expected for livermorium compared to the (relativistically) closed-shell elements copernicium (element 112) and flerovium (element 114) due to the presence of two unpaired $7p_{3/2}$-electrons. This is similar for nihonium (element 113) and moscovium with one unpaired $7p_{1/2}$ and $7p_{3/2}$ electron, respectively.[10] Theoretical studies suggest that the adsorption enthalpies of elemental livermorium and livermorium hydride on quartz are the same as those for elemental polonium and polonium hydride, respectively.[11] However, the volatility sequence of the oxides is predicted to increase in the order of $PoO_2 < PoO < Po$, which is different from the one predicted for the corresponding livermorium species ($LvO < LvO_2 < Lv$).[11] The general

[a] Johannes Gutenberg University Mainz, 55099, Mainz, Germany.
 E-mail: kahermai@uni-mainz.de
[b] GSI Helmholtzzentrum für Schwerionenforschung GmbH, 64291, Darmstadt, Germany
[c] Helmholtz Institute Mainz, 55099, Mainz, Germany
[d] Czech Technical University in Prague, 115 19, Prague, Czech Republic
[e] University of Oslo, 0315, Oslo, Norway
[f] Nuclear Physics Institute CAS, 250 68, Husinec-Řež, Czech Republic

This journal is © the Owner Societies 2026

Phys. Chem. Chem. Phys., 2026, **28**, 7617–7628 | 7617

similarity of the calculated volatilities of livermorium and polonium compounds underlines the importance of the studies of polonium as preparatory work for future studies of livermorium. The studies of oxidized polonium are particularly important, as the difference in the volatility trend of the oxides seems to provide a pathway for chemically distinguishing livermorium from polonium. Even if livermorium will be studied in the elemental state in future experiments, a reaction with oxygen impurities can never be fully excluded. This provides another motivation to study the oxides of polonium to provide a benchmark for future studies of livermorium. In the present study, we thus explore the adsorption of oxidized polonium onto quartz in detail.

In general, SHE nuclei often have very short half-lives and have to be produced atom by atom via heavy-ion fusion reactions.[8] Consequently, the chemical study of SHEs requires experimental approaches and strategies that enable the study of single atoms.[8] Gas–solid chromatography (GC) is the prime method for studying the gas-phase chemistry of SHEs and their homologues.[8,12] A common approach is thermochromatography, which uses a column along which a negative temperature gradient is applied. Single-atom quantities of the element under study are transported through the chromatography column by the carrier gas. The analysed species interact with the column material and will deposit at a specific temperature (called deposition temperature), determined by the adsorption enthalpy ($-\Delta H_{ads}$) of the chemical species on the column surface and by experimental conditions such as the gas flow rate.[13] From the experimentally measured deposition pattern and the deposition temperature, the adsorption enthalpy is determined using Zvára's Monte Carlo simulation,[14] which is based on the principle of mobile adsorption. The simulation takes the experimental parameters into account and has $-\Delta H_{ads}$ as the only free parameter. Multiple simulations are performed for different adsorption enthalpy values, and the results of the simulation are compared to the experimental results. The adsorption enthalpy of the simulation which matches the experimental results best is taken as the experimental value. The Monte Carlo method is a valuable approach for determining the adsorption enthalpy due to its flexibility and easy adaptability to specific experimental conditions.[15–17] However, the method relies on several assumptions and approximations that may not always hold true. For example, the assumption of simple reversible adsorption of molecules that are unaltered by the interaction with the surface is valid only when no chemical reactions occur between the studied species and the surface.[18] Typical experimental surface materials include gold or quartz.

To compare the chemical properties of SHEs to those of the other members of the group, similar gas chromatography experiments are performed with the lighter homologues of SHEs, usually under single-atom conditions.

Polonium, unlike the homologues of the lighter SHEs, is found only in trace amounts on Earth.[1] Thus, in this case also chemical studies with a lighter homologue of a SHE can be performed only with small amounts. Its chemical properties were explored in detail when milligram amounts of ^{210}Po were

produced in a nuclear reactor by irradiating ^{209}Bi.[19] Its chemical reactivity is similar to that of selenium and tellurium. Stable oxidation states include −II (as polonide), 0, +II, +IV and +VII, with the +IV state being the most stable one.[20,21] Polonium is insoluble in water but dissolves in acids (e.g. hydrochloric, nitric or sulfuric acid). Handling macroscopic amounts of polonium (especially ^{210}Po) introduces unique difficulties due to its high specific activity, which causes self-heating of samples and complicates temperature-dependent studies. Polonium is more metallic than tellurium, as evidenced by its positive temperature resistance coefficient, as well as its lower ionization energy and reduced electronegativity when compared to tellurium.[22]

Under standard conditions, metallic polonium oxidizes slowly in air, forming PoO_2, in which polonium is found in its most stable +IV oxidation state. The reaction becomes notably faster at temperatures above 250 °C.[23,24] In an argon atmosphere and in a vacuum, the dioxide decomposes into elements at 500 °C. The presence of oxygen seems to inhibit the decomposition.[25,26] The sublimation enthalpy of PoO_2 is reported to be $\Delta H_{sub}(PoO_2) = (65.3 \pm 2.3)$ kcal mol^{-1} ((273 ± 9.6) kJ mol^{-1}). However, the latter study also found support for a dissociative sublimation mechanism.[26] In addition to PoO_2, PoO and PoO_3 have been identified.[22,23] Neither of these compounds could be synthesised so far by the reaction of the elements in the gas phase.[20,22]

In addition to the oxides (anhydrides) mentioned above, the respective hydrated compounds, $Po(OH)_2$, H_2PoO_3 and $PoO_3\cdot aq$, exist. The structure of the latter compound is not known. As the anhydrides are not soluble in water, the corresponding hydroxide or oxo-acid has to be produced in reactions with bases.[20] $Po(OH)_2$ is the only dihydroxide known in the group of chalcogens and can be easily oxidized.[20,22]

Similar compounds (oxides as well as hydroxides) are also known for the lighter members of group 16 – sulphur, selenium and tellurium.[21] Since thermochromatography does not allow a direct speciation of the formed species, and the chemistry of polonium has only been little studied due to its high radiotoxicity, a comparison of its chemical properties with those of its lighter homologues can be beneficial.

Previously, gas chromatography experiments have already been conducted to study the reactivity of polonium towards various metal surfaces such as gold, platinum and silver and towards fused silica (SiO_2 or quartz).[4–6,27–31] In these works, the adsorption enthalpy of elemental polonium in inert or reducing atmospheres on quartz surfaces was found to be around 85 kJ mol^{-1} by B. Eichler et al.,[29] Vogt et al.[30] and Gärtner.[31] Recently, this value was confirmed.[32] In this latest study, it was also found that the degree of hydroxylation of the quartz surface significantly impacts the deposition pattern of polonium.[32] In general, the degree of hydroxylation of quartz glass depends on the production method of the glass and on the history between its production and use, i.e., how it was stored and potentially pretreated before use, e.g., by heating in a defined atmosphere. Exposure of the quartz glass to water or hydrogen can increase the degree of hydroxylation on the surface, whereas thermal pretreatment for several hours

7618 | Phys. Chem. Chem. Phys., 2026, **28**, 7617–7628

This journal is © the Owner Societies 2026

(at about 1000 °C) in an inert atmosphere reduces the amount of hydroxyl groups.[33,34] In general, hydroxyl groups on the surface of quartz can be grouped into three different categories: isolated, vicinal and geminal silanol groups. Vicinal silanol groups are at a sufficiently short distance to each other to engage in hydrogen bonding, in contrast to isolated silanol groups. In geminal silanol groups, two hydroxy groups are attached to only one silicon atom.[35,36] These hydroxyl groups can further serve as adsorption sites for the physisorption of water molecules *via* hydrogen bonds. The abundance of the different types of hydroxyl groups found on the surface probably depends on the processing history of the employed quartz glass.[36]

If quartz glass with a high degree of hydroxylation is used, polonium can react with the hydroxyl groups, forming a low-volatile compound which is likely an oxidized species.[32] A similar observation was also recently published for the deposition of astatine on quartz glass.[37]

Due to the complicated dependencies of the silanol concentration on the surface of quartz on the production method, the thermal history and the storage time and environment, we also investigated α-Al$_2$O$_3$ in this study as an alternative surface. Under normal conditions (20 °C and 50–60% humidity), the α-Al$_2$O$_3$ surface is fully hydroxylated, making it more similar to γ-Al(OH)$_3$ than to the bulk structure of α-Al$_2$O$_3$.[38–40] Similar to quartz glass, the OH-groups determine the reactivity of the surface with respect to the experiments discussed here. The OH-content on both surfaces can be reduced by annealing the material at high temperatures. The concentration of OH-groups on an α-Al$_2$O$_3$ surface is already noticeably reduced when the sample is heated above 400 °C. However, it is unclear if complete dehydroxylation of the surface is possible.[40,41] During annealing, first the density of neighbouring OH groups is reduced and Al–O–Al groups form.[42] Isolated OH-groups can only be removed at higher temperatures (1000 °C).[41] The chemical properties, and thus the exact temperature at which the OH-groups are removed, depend on the number of coordinated Al^{3+} ions.[39,41,43,44] A wide range of differently reactive OH-groups on the surface can be expected, especially for sintered α-Al$_2$O$_3$, since no defined surface termination exists.[40,42,45] As for quartz, the hydroxyl groups on the surface of α-Al$_2$O$_3$ can engage in hydrogen-bonding with each other if they are sufficiently close.[39] Also, they provide an adsorption site for molecular water *via* hydrogen-bonding. It is expected that up to three partially ordered monolayers of water can adsorb onto the surface under ambient conditions.[38] On both surfaces, the reactivity, polarity or structure of the surface can change significantly due to this adsorption of water.[46]

Here, we investigate the chemical interaction of elemental polonium and its oxidized species with quartz and α-Al$_2$O$_3$ surfaces using thermochromatography. Adding to the experiments from previous works,[28,32] in this study, we explored the behaviour of polonium in oxidizing atmospheres on quartz in detail. Also, we explored α-Al$_2$O$_3$ as an alternative stationary phase for gas chromatography experiments. The experiments

are conducted to lay a foundation for future chemical investigations of the superheavy element livermorium.

Experimental

Thermochromatography experiments involving radioactive nuclei can only be carried out in licensed laboratories under appropriate radiation protection regulations. Irradiation was performed at the CANAM infrastructure of the Nuclear Physics Institute of the Czech Academy of Sciences in Řež (Czech Republic) using the MARGE (Modular Robotic Gas-Jet Target System) beamline and a recoil transfer chamber.[47] All (technical) details regarding the used materials and the employed setup can be found in the SI.

^{204}Po and ^{205}Po were produced in the 4n and 5n evaporation channel of the fusion reaction of a 48-MeV ^{3}He beam with isotopically enriched ^{206}Pb targets. The target material was deposited on titanium backing foils (2.3 µm or 5 µm). We estimate that a few million polonium atoms can be produced per hour, not taking the radioactive decay of the atoms into account. Recoiling nuclei were collected in catcher foils which were placed in the chromatography column after the end of irradiation. These foils were composed of 2.5 µm-thick titanium or 75 µm-thick carbon. For all experiments, the used catcher material can be found in Table S1 of the SI. For each run, the irradiation time and the time that elapsed between the end of irradiation and the beginning of the experiment are also given in Table S1 of the SI.

The experimental setup used for thermochromatography is illustrated in Fig. 1. A carrier gas (pure helium or a mixture of helium and a reactive gas) transported single-atom quantities of polonium thermally released from the catcher foil through the chromatography column in which they interact with the surface.

The temperature gradient applied to the column was established using three tube furnaces at the beginning and copper coils with flowing cooling water at the end of the column. A mass flow meter and a pressure indicator (PI) were used at the end of the column to monitor the gas flow and the pressure in the column. Radioisotopes passing through the column were collected in an activated charcoal filter (Teflon tube having the same inner diameter as the quartz and α-Al$_2$O$_3$ columns and filled with activated charcoal).

The helium carrier gas (Linde, 99.9999%) was further purified by passing several cartridges to reduce water and oxygen impurities before it passed through the experimental setup. Oxygen (Linde, 99.995%) could be added to the carrier gas *via* a ball valve. In experiments with water as a reactive gas, a reservoir containing deionized water was connected to the gas system in front of the chromatography column. This reservoir was then heated to 55 °C to evaporate water directly into the helium and/or oxygen stream. The gas was led to the experiment using polyfluoroethylene or stainless-steel capillaries. The helium and oxygen gas flow rates were controlled with two mass flow controllers. The employed gas flow rates can be
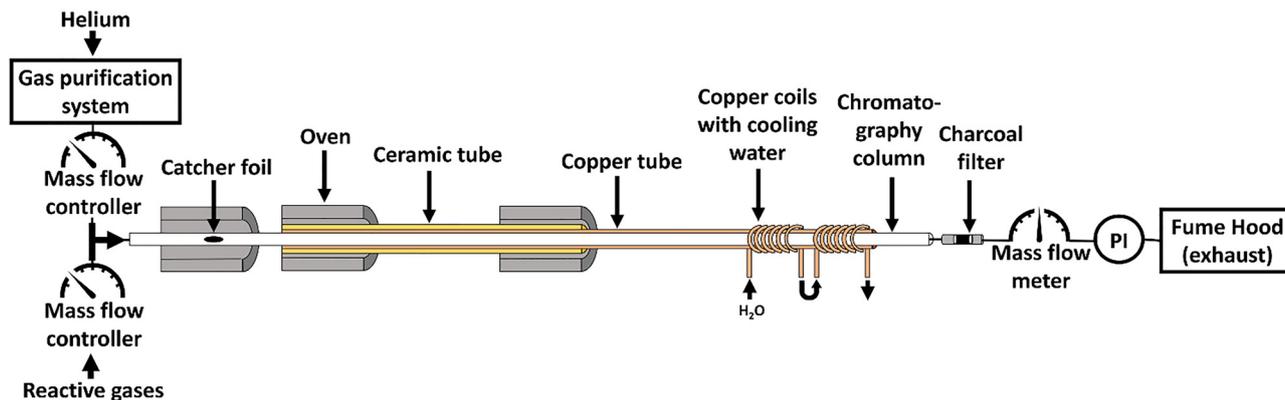
This journal is © the Owner Societies 2026

Phys. Chem. Chem. Phys., 2026, **28**, 7617–7628 | 7619

Fig. 1 Schematic of the thermochromatography setup used in this work. For detailed information, see the main text. Modified from ref. 32 with permission from the PCCP Owner Societies.

Table 1 Summary of adsorption enthalpies $-\Delta H_{ads}$ determined using the Monte Carlo simulation from the deposition temperatures T_{dep} in all experiments, as well as the most important experimental parameters and the species to which the deposition is assigned

Experiment	Gas atmosphere	Gas flow rate/sccm min^{-1}	Surface	T_{dep}/°C	$-\Delta H_{ads}$/kJ mol^{-1}	Assigned species
H2O$_{SiO2}$	He/H$_2$O^a	50	SiO$_2$	55 ± 5	80^{+3}_{-2}	Po
O2$_{SiO2}$ I	He/O$_2$ (4:1)	100	SiO$_2$	290 ± 10	≥ 137	PoO$_2$
				158 ± 5	105 ± 6	PoO/H$_2$PoO$_3$
				78 ± 5	87^{+3}_{-7}	Po
O2$_{SiO2}$ II	He/O$_2$ (4:1)	50	SiO$_2$	320 ± 7		PoO$_2$
				156 ± 5		PoO/H$_2$PoO$_3$
				64 ± 5		Po
O2$_{SiO2}$ III	O$_2$	100	SiO$_2$	380 ± 10		PoO$_2$
				138 ± 3		PoO/H$_2$PoO$_3$
				53 ± 3		Po
O2/H2O$_{SiO2}$	O$_2$/H$_2$O^a	100	SiO$_2$	153 ± 3		PoO/H$_2$PoO$_3$
				42 ± 3		Po
He$_{Al2O3}$	He	100	α-Al$_2$O$_3$	72 ± 3	85^{+4}_{-3}	Po

^{a} Water was directly evaporated into the helium/oxygen stream at 55 °C.

found in Table 1. The abbreviations for experiments used in the following discussions indicate the gas and the type of surface used. Here, He describes a gas atmosphere of 100% helium and H$_2$O or O$_2$ indicates that water or oxygen has been added to the gas phase. The type of surface (SiO$_2$ or α-Al$_2$O$_3$) is indicated as an index.

As chromatography columns, quartz glass and α-Al$_2$O$_3$ tubes were employed. The quartz glass tubes were recently produced by electro-melting of quartz granulate in a vacuum and were additionally annealed at 1000 °C for 20 h in an inert gas atmosphere before the experiment. For experiments on α-Al$_2$O$_3$, ceramic corundum tubes which were annealed at 1000 °C in an inert gas atmosphere for 10 h before the experiment were used.

For each experiment, the catcher foil was introduced into the column at the hottest point. The carrier gas was flushed through the heated column for 1–2 h (corresponding to the experiment time, see Table S1) with the carrier gas (and reactive gas) running. Before the experiment, the γ spectrum of the catcher foil containing the accumulated polonium activity was measured with a HPGe-detector to identify the implanted reaction products. During the experiment, the oven temperatures,

the pressure and the gas flow rate were continuously monitored. After the experiment, the gas flow was stopped, and the column was removed from the furnaces through the cold end and sealed with septum caps. After cooling down to room temperature, the quartz glass columns were cut into (2.0 ± 0.2) cm or (4.0 ± 0.2) cm pieces. Each sample was sealed in a plastic vial. Subsequently, the samples, the activated charcoal filter, and the catcher foil were measured with a HPGe-detector. For this, a 3D-printed sample holder was used to ensure consistent measurement geometry. The α-Al$_2$O$_3$ columns were not cut. Thus, γ ray measurements of these columns were conducted by scanning the column using a custom lead collimator with a 2 cm wide aperture in front of the detector.

The temperature gradient was measured after each experiment in 2-cm or 4-cm steps depending on the local steepness of the gradient, using a 100 cm-long type-K thermocouple attached to a read-out unit. The temperature error was estimated from the uncertainty of the read-out unit (0.05%) and the thermocouple (±2 °C) as specified by the manufacturers and from the uncertainty of the placement of the thermocouple (±5 mm). As the temperature gradient became steeper towards higher temperatures, the uncertainty of the placement of the

7620 | *Phys. Chem. Chem. Phys.,* 2026, **28**, 7617–7628

This journal is © the Owner Societies 2026

thermocouple causes a larger temperature error at these higher temperatures.

To obtain thermochromatograms, the γ lines and X-rays originating from the decay of ^{204}Po (884 keV; I_γ = 29.9%, 1016 keV; I_γ = 24.1%, 77.108 keV; and I_X = 73.0%) and of ^{205}Po (872 keV; I_γ = 37.0%, 1001 keV; and I_γ = 28.8%) were integrated in the γ spectra of all individual column segments. They were then baseline-, dead time- and decay-corrected and normalized to the measurement time. To obtain the relative deposition yields of individual 2-cm or 4-cm long parts of a column, the obtained net peak areas were normalized to the total polonium activity in the column. The uncertainty in the length of the column segments resulting from the cutting of the chromatography column or the placement of the column in the lead collimator was added to the error of the net peak area. The deposition patterns obtained from the evaluation of the different γ lines were compared to each other to ensure that the evaluated deposition was not influenced by any other radioisotopes. In the thermochromatograms measured on quartz glass columns shown in this work, the deposition pattern evaluated from the strongest γ line of the longer-lived and more abundantly produced ^{204}Po is displayed, as this γ line proved to be undisturbed. In experiments using α-Al$_2$O$_3$ columns, the deposition pattern was evaluated from the X-ray line at 77.108 keV to minimize the influence from neighbouring column parts, as low energies can be better shielded by the lead collimator. In experiment H2O$_{SiO2}$, the column was only measured in 4-cm steps between 38 and 60 centimetres. To obtain the deposition of polonium activity per 2 cm, it was assumed that the activity is equally distributed in the 4-cm pieces.

The adsorption enthalpy was determined by comparing experimental results with distributions generated through Monte Carlo simulations (MCS),[14] using the experimental parameters as input data. The most likely value of the adsorption enthalpy was derived from the simulated distribution that best matched the experimental observations. For the error analysis of the adsorption enthalpy, fluctuations and errors of experimental parameters such as the gas flow rate or the temperature were taken into account.

A key parameter in the Monte Carlo simulation is the time the atoms remain in the column.[14] For chromatography experiments, where the experiment time is longer than the lifetime of the radioisotope under study, this duration is equal to the lifetime value which is randomly selected from the lifetime distribution. In chromatography experiments where the experiment duration is shorter than or comparable to the half-life, the activity distribution can be measured after the experiment. In this case, the "lifetime" – more accurately termed "sojourn time" – is not defined by the nuclide's half-life. Instead, it is determined as the time difference between an atom's entry into the column and the experiment's end. In the experiments carried out in this work, the entry time is defined by the release of polonium from the catcher foil, induced by heating the foil. Due to varying implantation depths and the distribution of diffusion velocities of polonium atoms within the catcher foil, the release of individual atoms occurs at different times.

This creates a distribution of sojourn times. Based on separate experiments investigating the release of polonium from the catcher foil, it was assumed that all atoms are released from the foil within approximately 5–10 minutes (depending on the temperature) after the start of the experiment. To account for atoms released either immediately at the start of the experiment or later during the experiment, the adsorption enthalpy was also calculated for the upper and lower bounds of the sojourn time. Any deviation in the adsorption enthalpy from the value obtained using the most probable sojourn time was added to the error margin of the final adsorption enthalpy.

Results and discussion

In all the described experiments with different gas compositions, thermochromatograms of polonium were obtained.

Table 1 summarizes the most important experimental parameters, the results for all conducted thermochromatography experiments and also the assignments of the measured deposition peaks to the most probable species.

Experiments in SiO$_2$ columns

In experiment H2O$_{SiO2}$, the deposition pattern of polonium in moist helium was examined. Fig. 2 shows the obtained chromatogram of polonium on quartz glass in this atmosphere.

In this experiment, the main deposition peak was observed at (55 ± 5) °C comprising (92 ± 4)% of the total polonium activity. This deposition temperature corresponds to the temperature at which water was evaporated into the helium stream to saturate the gas with water. The remaining polonium activity, which is not part of the main deposition peak, was deposited in a flat distribution starting from a temperature of (227 ± 5) °C down to the main deposition peak. An adsorption enthalpy of $-\Delta H_{ads}(Po) = 80^{+3}_{-2}$ kJ mol^{-1} was determined for the deposited species from the main deposition peak using the
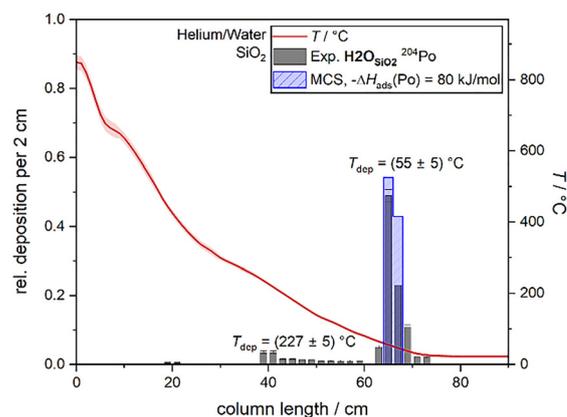

Fig. 2 Thermochromatogram of ^{204}Po in moist helium on quartz glass. The experimental depositions are shown in grey, the simulated deposition using the Monte Carlo simulation (MCS) is shown in blue and the temperature gradient is shown in red. The relative area of the simulated deposition was scaled to the relative area of the experimental peaks. Here, $-\Delta H_{ads}$ is the adsorption enthalpy and T_{dep} is the deposition temperature at the peak maximum.

This journal is © the Owner Societies 2026

Phys. Chem. Chem. Phys., 2026, **28**, 7617–7628 | **7621**

Monte Carlo method. The determined adsorption enthalpy is thus slightly lower but still in agreement with the adsorption enthalpy of elemental polonium ($-\Delta H_{ads}$(Po) = 85^{+3}_{-2} kJ mol^{-1}).[32] This indicates the deposition of elemental polonium at (55 ± 5) °C. However, it cannot be excluded that water vapour was also deposited on the surface of the chromatography column. Thus, the determined adsorption enthalpy might describe the deposition of polonium on water and not on quartz.

The experiment indicates that polonium does not undergo gas-phase reactions with water vapour to form species less volatile than elemental polonium under the selected experimental conditions. This is consistent with previous observations that elemental polonium does not form other species, such as oxides, when exposed to water at room temperature.[20] Although the added water vapour might not react directly with polonium, it is known that water can alter the quartz surface by (dissociative) adsorption, thereby increasing the density of hydroxyl groups on the surface.[33,48] The hydroxyl concentration on initially unreactive quartz glass with a low hydroxyl concentration was shown to increase upon exposure to water at high temperatures (800–1000 °C), eventually reaching an equilibrium concentration.[33,48] Although the high temperatures necessary for the reaction of quartz with water were reached at the beginning of the column in this experiment, the comparatively short experimental duration (104 min) limits the concentration of the eventually formed hydroxyl groups. Still, surface modifications through the interaction of the quartz surface with water can significantly alter the properties of the surface through, e.g., physisorption of water molecules.

The deposition from (227 ± 5) °C onwards observed in this experiment does not represent an adsorption peak that can be described by the model of mobile adsorption. Thus, it seems unlikely that a stable, second species was formed. The deposition can probably rather be described by a different interaction of polonium with the surface altered by water.

In experiments O2$_{SiO2}$ I to O2$_{SiO2}$ III, the deposition of polonium transported in an oxygen-containing atmosphere was evaluated. In experiment O2$_{SiO2}$ I, an oxygen content of 20% and a temperature gradient starting at relatively low temperatures was employed. The measured thermochromatogram is depicted in Fig. 3.

Three rather broad deposition zones were observed in experiment O2$_{SiO2}$ I: a high temperature deposition zone directly at the beginning of the chromatography column starting from (290 ± 10) °C with (5 ± 2)% of the polonium activity, a deposition zone at moderate temperatures with a maximum at (158 ± 5) °C with (29 ± 5)% of the activity, and a low temperature deposition zone with a maximum at (78 ± 5) °C containing the majority – (66 ± 5)% – of the activity. By comparing the patterns of the three deposition zones, it becomes obvious that the activity in the high temperature deposition zone cannot be described as a peak but rather resembles a pattern obtained by diffusion-controlled deposition.

Correspondingly, only the lower limit of the adsorption enthalpy of this deposited species can be determined using the Monte Carlo method. The best fit to the experimental data
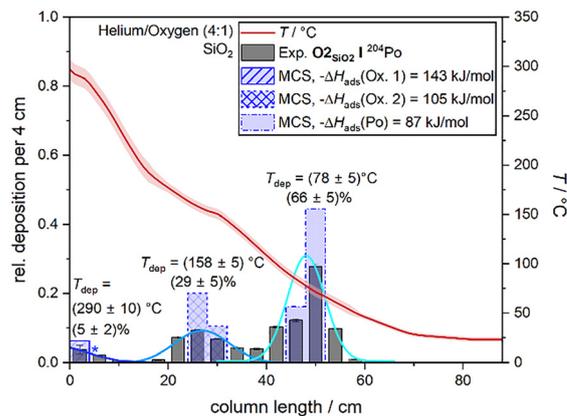

Fig. 3 Thermochromatogram of [204]Po in a helium/oxygen (4 : 1) atmosphere on quartz glass. The experimental depositions are shown in grey, the simulated deposition using the Monte Carlo simulation (MCS) is shown in blue and the temperature gradient is shown in red. The relative area of the simulated deposition was scaled to the relative area of the experimental peaks. Here, $-\Delta H_{ads}$ is the adsorption enthalpy and T_{dep} is the deposition temperature at the peak maximum. All peaks (except for the high-temperature peak marked with an asterisk) were fitted with Gauss functions to determine the relative amount of polonium activity deposited in each peak (blue lines). The function marked with an asterisk is shown for clarity. In this case, the amount of activity was determined as the sum of the activities in the first peak at high temperatures.

was found for an adsorption enthalpy of $-\Delta H_{ads}$(Ox. 1) = 143 kJ mol^{-1}. In order to obtain the lower limit of the adsorption enthalpy, the negative error of this adsorption enthalpy was subtracted from the determined value. This resulted in a lower limit of $-\Delta H^{limit}_{ads}$ (Ox. 1) $\geq$ 137 kJ mol^{-1} for the species deposited in the high-temperature zone. For the species deposited at (158 ± 5) °C, an adsorption enthalpy of $-\Delta H_{ads}$(Ox. 2) = (105 ± 6) kJ mol^{-1} was determined using the Monte Carlo method. Analogously, an adsorption enthalpy of $-\Delta H_{ads}$(Po) = 87^{+3}_{-7} kJ mol^{-1} was found for the species deposited in the low-temperature zone. This adsorption enthalpy is in agreement with the value assigned to elemental polonium in previous measurements in pure[32] and moist helium atmospheres. Thus, in accordance with ref. 32, we assign the peak at (78 ± 5) °C to the deposition of elemental polonium. In contrast to the previously reported experiments conducted in a pure helium atmosphere where only one peak was detected and assigned to elemental polonium,[32] two additional chemical species were observed in the oxygen atmosphere in our experiments. Considering the employed gas atmosphere, these species are most probably oxygen-containing polonium species which were formed by a chemical reaction with oxygen.

In contrast to experiment H2O$_{SiO2}$, where experimental and simulated distributions exhibited the same width, this is not the case in experiment O2$_{SiO2}$ I. Rather, the experimental distribution is significantly wider. This is a sign that the deposition pattern measured in experiment O2$_{SiO2}$ I deviates from the model of mobile adsorption and that the oxidation of polonium influences the deposition pattern. Thus, the Monte Carlo model by Zvára might not be applicable for this

7622 | *Phys. Chem. Chem. Phys.*, 2026, **28**, 7617–7628

This journal is © the Owner Societies 2026

experiment. As this was observed for all experiments in the oxygen-containing atmosphere, the adsorption enthalpies of the deposited species were not determined in the following experiments. Since, however, the experimental conditions (experiment time and gas flow rate, see Table 1 and Table S1) are very similar in all the experiments conducted in this work, the deposition temperature can be used to compare the experiments with each other.

In experiment $O2_{SiO2}$ II, the same gas composition as in experiment $O2_{SiO2}$ I was used, but a temperature gradient with a higher starting temperature was applied to the column. The measured thermochromatogram is shown in Fig. 4.

As in experiment $O2_{SiO2}$ I, multiple deposition zones can be observed in the column. The high temperature deposition peak shows a maximum at (320 ± 7) °C and the deposition zone at moderate temperatures exhibits a maximum at (156 ± 5) °C. As in the previous experiment, a fraction $((5 \pm 1)\%)$ of the polonium activity deposited at low temperatures with a maximum at (64 ± 5) °C. Thus, as in experiment $O2_{SiO2}$ I, three different chemical species were observed in experiment $O2_{SiO2}$ II. However, the fraction of total activity measured at these lower temperatures (between 50 and 60 °C) decreased significantly by about 60 percentage points compared to experiment $O2_{SiO2}$ I. In contrast, the fraction of activity measured in the high-temperature deposition zone significantly increased by about the same extent as the amount of activity in the low-temperature zone decreased. The fraction of the polonium activity deposited at moderate temperatures (about 30%) is roughly the same as in experiment $O2_{SiO2}$ I.

The only difference between experiment $O2_{SiO2}$ II and experiment $O2_{SiO2}$ I was the higher starting temperature applied to the column in experiment $O2_{SiO2}$ II. A change in the deposition pattern only due to a change in the applied temperature cannot be explained in the frame of the theory of mobile adsorption. The different distributions of activity in experiment $O2_{SiO2}$ II compared to that in experiment $O2_{SiO2}$ I are thus an indication that a chemical reaction is superimposed on the chromatography process and the yield of the proceeding chemical reaction is dependent on the temperature. This can be observed in the increased amount of polonium activity deposited in the high-temperature deposition zone in experiment $O2_{SiO2}$ II when compared to experiment $O2_{SiO2}$ I, as the higher temperature leads to an increased formation of one of the formed, presumably oxygen-containing, polonium species. Accordingly, the amount of polonium activity deposited in the low-temperature zone, previously assigned to elemental polonium in experiment $O2_{SiO2}$ I, has significantly decreased in experiment $O2_{SiO2}$ II compared to experiment $O2_{SiO2}$ I. This can be explained with an increasing oxidation of elemental polonium due to the higher temperature. Thus, in accordance with experiment $O2_{SiO2}$ I, we assign the species deposited in the low-temperature zone in experiment $O2_{SiO2}$ II also to elemental polonium.

In experiment $O2_{SiO2}$ III, the oxygen content in the gas phase was increased to 100%. The obtained thermochromatogram is depicted in Fig. 5.

The obtained chromatogram again shows broadly three deposition zones. In this experiment, the high-temperature deposition zone with about $(60 \pm 20)\%$ of the polonium activity exhibits a maximum at (380 ± 10) °C. The deposition peak at moderate temperatures with about $(30 \pm 20)\%$ of the activity shows a maximum at (138 ± 3) °C. The low-temperature deposition zone has a maximum at (53 ± 3) °C and contains about $(5 \pm 2)\%$ of the activity. Compared to experiment $O2_{SiO2}$ II, the fraction of activity deposited in the different zones did not change significantly.

To study the influence of water on the deposition pattern of oxidized polonium, water was evaporated into the oxygen gas flow in experiment $O2/H2O_{SiO2}$ in the same way as in
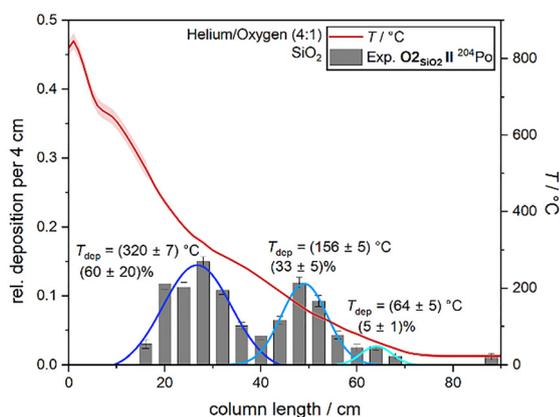

Fig. 4 Thermochromatogram of ^{204}Po in a helium/oxygen $(4:1)$ atmosphere on quartz glass. In comparison to experiment $O2_{SiO2}$ I, a temperature gradient with a higher starting temperature was applied to the column. The experimental depositions are shown in grey and the temperature gradient is shown in red. Here, T_{dep} is the deposition temperature at the peak maximum. All peaks were fitted with Gauss functions to determine the relative amount of polonium activity deposited in each peak (blue lines).
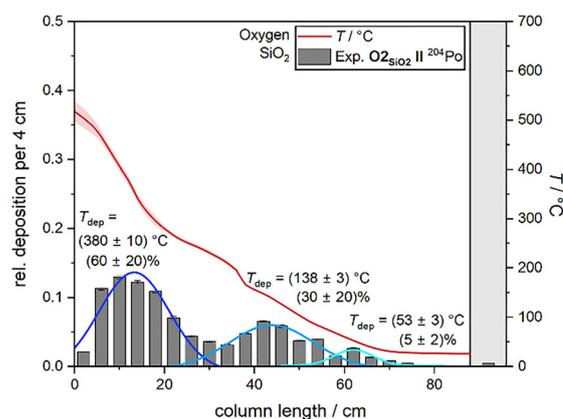

Fig. 5 Thermochromatogram of ^{204}Po in an oxygen atmosphere on quartz glass. The experimental depositions are shown in grey and the temperature gradient is shown in red. Here, T_{dep} is the deposition temperature at the peak maximum. All peaks were fitted with Gauss functions to determine the relative amount of polonium activity deposited in each peak (blue lines). The amount of activity which reached the activated charcoal filter is shown on a grey background on the right.
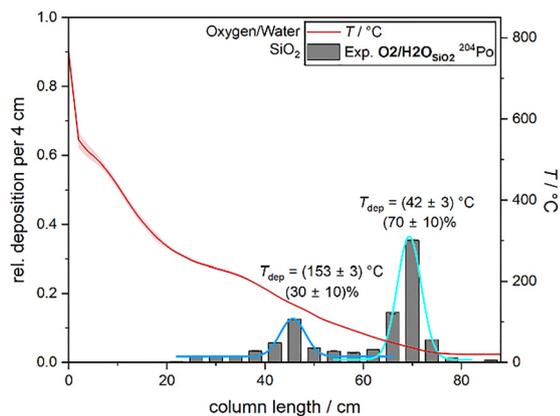
This journal is © the Owner Societies 2026

Phys. Chem. Chem. Phys., 2026, **28**, 7617–7628 | **7623**

Fig. 6 Thermochromatogram of ^{204}Po in a moist oxygen atmosphere on quartz glass. The experimental depositions are shown in grey and the temperature gradient is shown in red. Here, T_{dep} is the deposition temperature at the peak maximum. All peaks were fitted with Gauss functions to determine the relative amount of polonium activity deposited in each peak (blue lines).

Table 2 Summary of all peak ratios and deposition temperatures in all experiments in the oxygen-containing atmosphere. Here, peak 1 corresponds to the high-temperature deposition peak, peak 2 to the deposition peak at intermediate temperatures and peak 3 to the low-temperature deposition peak

	O2$_{SiO2}$ I	O2$_{SiO2}$ II	O2$_{SiO2}$ III	O2/H2O$_{SiO2}$
Peak 1	(290 ± 10) °C (5 ± 2)%	(320 ± 7) °C (60 ± 20)%	(380 ± 10) °C (60 ± 20)%	
Peak 2	(158 ± 5) °C (29 ± 5)%	(156 ± 5) °C (33 ± 5)%	(138 ± 3) °C (30 ± 20)%	(153 ± 3) °C (30 ± 10)%
Peak 3	(78 ± 5) °C (66 ± 5)%	(64 ± 5) °C (5 ± 1)%	(53 ± 3) °C (5 ± 2)%	(42 ± 3) °C (70 ± 10)%

experiment H2O$_{SiO2}$. The measured thermochromatogram is depicted in Fig. 6.

In experiment O2/H2O$_{SiO2}$, a majority – (70 ± 10)% – of the polonium activity was deposited in a broad deposition peak with a maximum at (42 ± 3) °C. This peak is in the vicinity of the low-temperature deposition zone also observed in the experiments with dry oxygen-containing atmosphere. The remaining activity was deposited with a flat and very broad deposition pattern starting from a temperature of (287 ± 6) °C down to the low-temperature deposition zone. This deposition zone exhibits a maximum at (153 ± 3) °C and is thus in the vicinity of the intermediate deposition zone observed in experiments O2$_{SiO2}$ I to O2$_{SiO2}$ III.

On the basis of the previous experiments, the species deposited at (42 ± 3) °C is again attributed to elemental polonium. As in the experiments in the dry oxygen-containing atmosphere discussed before, especially the experimental deposition zone at moderate temperatures is very broad. This again hints at a chemical reaction that is superimposed on the chromatography process. Compared to the experiments conducted in the dry oxygen-containing atmosphere, in experiment O2/H2O$_{SiO2}$ the high-temperature deposition zone is missing.

Throughout all conducted experiments, a total of three different chemical species were observed. The yield of these chemical species was found to be dependent on the highest applied temperature and the composition of the gas phase.

On the basis of all the previously discussed experiments, the species deposited in the low-temperature deposition zone in experiments O2$_{SiO2}$ I to O2$_{SiO2}$ III and experiment O2/H2O$_{SiO2}$ is assigned to elemental polonium.[32] A summary of the peak ratios and deposition temperatures of all peaks of all experiments in the oxygen atmosphere can be found in Table 2.

As described in the Introduction, PoO$_2$ is the only known oxide of polonium that can be formed from the elements. The reaction takes place rapidly at temperatures above 250 °C.[22,23] Thus, it seems likely that PoO$_2$ was formed by the chemical

reaction with oxygen in the gas phase or on the surface of the (probably O$_2$-covered) catcher foil during our experiments. In experiment O2$_{SiO2}$ I, the maximum temperature applied to the column was only (290 ± 10) °C which is only slightly above the reaction temperature. Thus, it can be expected that PoO$_2$ was formed with a lower chemical yield compared to the other experiments with the oxygen-containing atmosphere, where regions with higher temperatures were present. This is indeed observed in the increase of the fraction of polonium activity deposited in the high-temperature deposition zone when comparing experiments O2$_{SiO2}$ I (lower temperature) and O2$_{SiO2}$ II (higher temperature). At the same time, a decrease in the fraction of elemental polonium is observed if a temperature gradient starting at higher temperatures is applied to the column. This indicates the deposition of PoO$_2$ in the high-temperature zone of the experiments.

Similar to a higher temperature, the higher oxygen concentration in experiment O2$_{SiO2}$ III should also lead to increased oxidation of polonium. However, this effect is not visible in the measured thermochromatograms. It is very likely that the oxidation of polonium already occurs on the surface of the catcher foil. The catcher foil will be covered by an O$_2$-layer, even at a share of only 20% oxygen in the gas phase. As a result, the oxygen concentration does not influence the proceeding chemical reaction.

Before assigning the deposition zone at moderate temperatures in experiments O2$_{SiO2}$ I to O2$_{SiO2}$ III and experiment O2/H2O$_{SiO2}$ to a distinct polonium species, the results of our experiments are compared to the known properties of oxygen-containing compounds of the lighter homologue tellurium.

When studying macroscopic amounts of tellurium, clusters of the form Te$_i$ (whereby i = 2–7) rather than individual atoms sublimate. The sublimation enthalpy was reported to be (158.6 ± 6.6) kJ mol^{-1} for Te$_2$ and (236.5 ± 15.9) kJ mol^{-1} for Te$_7$.[49] Since TeO could not be isolated in the solid state, no experimental data on its sublimation enthalpy exist. The sublimation enthalpy of TeO$_2$ is reported to be (59 ± 2) kcal mol^{-1} $((247 \pm 9)$ kJ mol$^{-1})$.[50] Accordingly, TeO$_2$ is less volatile than the element. This was also observed in thermochromatography experiments with tellurium on quartz by Maugeri *et al.*[51] This strengthens the previous assignment of the species deposited in the high-temperature deposition zone to PoO$_2$, as the

7624 | *Phys. Chem. Chem. Phys.*, 2026, **28**, 7617–7628

This journal is © the Owner Societies 2026

deposited species is significantly less volatile than elemental polonium. TeO_2 is known to react with water at temperatures above 600 °C forming the corresponding oxoacid H_2TeO_3. However, the compound is reported to be stable only in the presence of water. Otherwise, it decomposes readily into TeO_2 and H_2O at higher temperatures.[50] Thermochromatography experiments with tellurium on quartz[51] point to a higher volatility of the oxyhydroxides compared to TeO_2.

For polonium, the corresponding acid H_2PoO_3 is also known.[22]

To assign the deposition zone at moderate temperatures in experiments $O2_{SiO2}$ I to $O2_{SiO2}$ III and experiment $O2/H2O_{SiO2}$ to a distinct polonium species, two different interpretations can be discussed:

• An assignment of the three deposition zones to the increasingly more volatile compounds $PoO_2 < PoO < Po$.

• A stepwise reaction, in which PoO_2 is first formed from the reaction of polonium with oxygen, which then reacts further with water or silanol groups on the surface to form an oxoacid (most probably H_2PoO_3).

The first interpretation is supported by the fact that in experiments with macroscopic amounts (up to milligrams) at elevated temperatures, PoO_2 was only stable in the presence of oxygen.[25] Also, the sublimation of the compound was reported to be connected to a dissociative mechanism.[26] The formation of the deposition zones at moderate temperatures could thus be explained by the decomposition of PoO_2, either in the gas phase or – more likely – on the surface. A similar mechanism has already been described for the deposition of ruthenium oxides on quartz.[52] The products of this decomposition (most likely PoO or Po) are expected to be more volatile than PoO_2. They would then be transported further through the column. This interpretation is in agreement with fully relativistic quantum-chemical calculations, which predict the volatility sequence $PoO_2 < PoO < Po$.[11] If water is added, a possible decomposition of PoO_2 on the surface might be favoured due to an *in situ* modification of the quartz surface during the experiment.

Alternatively, the observed deposition patterns could also be explained by a stepwise reaction, in which PoO_2 is initially formed by the reaction of polonium with oxygen. In the following step, PoO_2 reacts with water or silanol groups on the surface forming the corresponding oxoacid H_2PoO_3. Since the presence of water as an impurity in the used oxygen gas is likely, such a reaction is also possible in the experiments where no water was explicitly added to the gas phase. However, the concentration of water in experiment $O2/H2O_{SiO2}$ is many orders of magnitude higher than that in experiments $O2_{SiO2}$ I to $O2_{SiO2}$ III. Thus, quantitative conversion of PoO_2 to H_2PoO_3 is plausible in experiment $O2/H2O_{SiO2}$.

Since thermochromatography does not allow a direct speciation of the deposited compound, the observed deposition peak at moderate temperatures cannot unambiguously be assigned to specific species. Also, the implementation of other analytical methods such as mass measurements is not possible due to the single-atom nature of the experiments. From the above

discussed aspects, it is plausible that PoO and/or H_2PoO_3 are present during our experiments.

In isothermal chromatography experiments in an oxygen-containing atmosphere conducted by R. Eichler *et al.*, the adsorption enthalpy of polonium, presumably as PoO_2, on quartz was evaluated to be 177 kJ mol^{-1}.[53] In thermochromatography studies by Maugeri *et al.*, the adsorption enthalpy of presumably PoO_2 on quartz was determined to be (215 ± 5) kJ mol^{-1}.[28] These values would transfer to deposition peaks with maxima at (420 ± 30) °C (177 kJ mol^{-1}) and (560 ± 30) °C $((215 \pm 5)$ kJ $mol^{-1})$ in our experiments. These temperatures are higher than the measured average of (330 ± 50) °C for the least volatile species observed in our experiments. Thus, no species interacting with an adsorption enthalpy of ≥ 177 kJ mol^{-1} was observed in our experiments. However, it is suspected that the deposition of oxidized polonium does not occur *via* mobile adsorption, as the chromatography process seems to be superimposed by a chemical reaction. Consequently, the Monte Carlo method by Zvára is not applicable and the adsorption enthalpies of oxidized polonium species determined under different experimental conditions in different experiments are likely not comparable. Further support for the interpretation that transport occurs in the form of a transport reaction[35] comes from the observation by Maugeri *et al.* They observed that their measured deposition peaks of polonium in an oxygen atmosphere were also significantly wider than the simulated distributions.[28] This is typical for a chromatography process superimposed by a chemical reaction.[35,54] In addition, they also found that through the addition of water to the oxygen atmosphere, a more volatile species is formed.[28] We cannot exclude that different surface modifications influence the proceeding reactions of polonium during chromatography. Thus, in our experiments, we only employed quartz columns which were thermally pretreated (dehydroxylated) to minimize surface effects.[32]

Experiments in α-Al₂O₃ columns

To explore an alternative stationary phase to quartz and to study the influence of the surface in general, experiments were performed not only on quartz glass but also on α-Al_2O_3. The experiment on α-Al_2O_3 was conducted in a pure helium atmosphere. The resulting thermochromatogram is shown in Fig. 7.

Only one deposition peak at (72 ± 3) °C was observed in the chromatography column. Thus, we conclude that only one species was present during the experiment. By utilizing the Monte Carlo simulation, an adsorption enthalpy of $-\Delta H_{ads}(Po) = 85^{+4}_{-3}$ kJ mol^{-1} could be determined. This is in agreement with the adsorption enthalpy value of elemental polonium on quartz.[32]

To be able to compare the experiments on quartz glass and α-Al_2O_3, it must be taken into account that the here employed α-Al_2O_3 columns exhibit a different surface roughness than the employed quartz glass columns. A higher roughness increases the real solid–gas interfacial area and thus also influences the adsorption–desorption cycle. To measure the surface roughness and the increase of surface area due to roughness, the
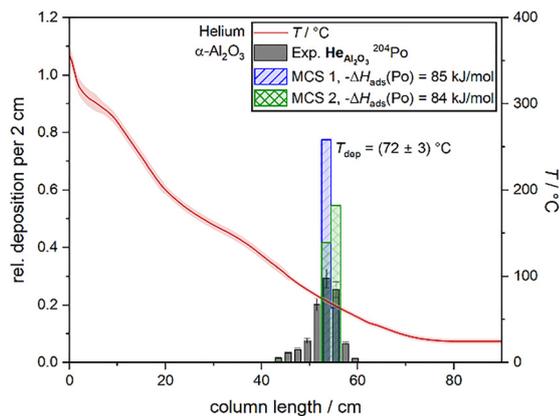
This journal is © the Owner Societies 2026

Phys. Chem. Chem. Phys., 2026, **28**, 7617–7628 | **7625**

Fig. 7 Thermochromatogram of ^{204}Po in a helium atmosphere on α-Al$_2$O$_3$. The experimental depositions are shown in grey, the simulated deposition using the unmodified Monte Carlo simulation (MCS) is shown in blue and the temperature gradient is shown in red. In green, a second MCS is shown where the roughness of the surface was taken into account Here, $-\Delta H_{ads}$ is the adsorption enthalpy and T_{dep} is the deposition temperature at the peak maximum.

Table 3 Projected A_{proj} (assuming a perfectly smooth surface over the measured area of 144.7 μm × 108.5 μm) and roughness-induced real surface area A_{real} for quartz glass and α-Al$_2$O$_3$. The factor F describes the ratio of real surface area to projected surface area

Surface	$A_{proj}/\mu m^2$	$A_{real}/\mu m^2$	F
Quartz glass	15 700	15800 ± 20	1.006 ± 0.001
α-Al$_2$O$_3$	15 700	19300 ± 200	1.23 ± 0.01

surfaces of the employed quartz and α-Al$_2$O$_3$ materials were characterized using a KEYENCE VK-X3000 Series Confocal Laser Scanning Microscope. The experimental details, the images taken, and the roughness parameters derived from the images can be found in the SI. Table 3 lists the projected surface area (assuming a perfectly smooth surface over the measured area of 144.7 μm × 108.5 μm) and the mean, roughness-induced real surface area (averaged over two measuring points) for quartz glass and α-Al$_2$O$_3$, as well as the ratio F of the real to the projected surface area. The surface area values reported here describe the roughness-induced increase of the real surface area of the scanned regions and should not be confused with mass-normalized specific surface areas.

From the data in Table 3, it can be concluded that the α-Al$_2$O$_3$ exhibits a significantly larger surface roughness compared to the quartz. Thus, the effective surface area is, compared to a perfectly smooth surface, increased by a factor of 1.23 ± 0.01. For quartz glass, the real surface area increases only by a factor of 1.006 ± 0.001 due to surface roughness. The Monte Carlo simulation assumes a perfectly smooth surface and calculates the surface area for tubular columns based on the lateral surface of a cylinder. As suggested by Zvára, the increase in surface area due to roughness can be taken into account if the nominal surface area is multiplied by the above-mentioned factors.[14] The adsorption enthalpy which was

determined while taking this factor into account is shown in Fig. 7 in green. By taking the surface roughness into account, the adsorption enthalpy of polonium on α-Al$_2$O$_3$ is reduced by only 1 kJ mol^{-1} compared to the Monte Carlo simulation which does not include the factor (blue). This is a negligible deviation when considering the found error interval. Thus, the adsorption enthalpies determined on quartz and on α-Al$_2$O$_3$ can be compared with each other.

By using helium as the carrier gas, it can be assumed that no reactions took place in the gas phase in experiment He$_{Al2O3}$. Reactions during the thermal release of the polonium from the catcher foil are also unlikely, as a low temperature and a carbon catcher were used in this experiment. In contrast to a catcher made of titanium, it can be assumed that fewer oxygen impurities are adsorbed onto carbon. Thus, the most probable species deposited at (72 ± 3) °C in experiment He$_{Al2O3}$ is elemental polonium.

The agreement of the adsorption enthalpies of elemental polonium on unreactive quartz and α-Al$_2$O$_3$ surfaces suggests that a similar adsorption mechanism takes place on both surfaces. This is somewhat surprising at first glance in view of the significantly different bonding in bulk SiO$_2$ (mostly covalent) and Al$_2$O$_3$ (more ionic).[46] This result thus might point to an adsorption of polonium onto the hydroxyl groups on the surface, which remain even after a high temperature treatment. However, it should be noted that surface polarity is not an intrinsic material constant but strongly depends on surface termination, reconstruction, and local coordination.[55] In the present study, both amorphous quartz glass and sintered α-Al$_2$O$_3$ exhibit structurally heterogeneous surfaces without a well-defined crystallographic termination. Thus, a definitive conclusion about the adsorption site of polonium cannot be drawn on the basis of the present results.

Conclusions

Thermochromatography experiments of polonium were conducted in helium and water- and oxygen-containing atmospheres on quartz glass, as well as on α-Al$_2$O$_3$.

In a moist helium atmosphere on quartz glass, an adsorption enthalpy of $-\Delta H_{ads}(Po) = 80^{+3}_{-2}$ kJ mol^{-1} was determined, which is the same as the adsorption enthalpy of elemental polonium reported earlier.[32] Thus, we conclude that elemental polonium does not directly react with water vapours up to 800 °C to form a fewer volatile species than elemental polonium. In experiments in an oxygen-containing atmosphere on quartz, at least two oxidized species were identified. The chemical yield of these compounds, probably formed by the reaction with oxygen, was found to be dependent on the temperature and the water content in the carrier gas. The less volatile oxygen-containing species was assigned to PoO$_2$. It is likely that PoO$_2$ formed from the reaction of polonium with oxygen can either decompose to form PoO or further react to form H$_2$PoO$_3$. Both interpretations are in line with the known chemistry of the lighter homologue tellurium.

7626 | *Phys. Chem. Chem. Phys.*, 2026, **28**, 7617–7628

This journal is © the Owner Societies 2026

The enthalpy of adsorption of elemental polonium onto α-Al_2O_3 in a helium atmosphere was determined to be $-\Delta H_{ads}(Po) = 85^{+4}_{-3}$ kJ mol^{-1}. This adsorption enthalpy value is in agreement with the adsorption enthalpy of elemental polonium on quartz glass.[32] This agreement suggests that on both surfaces, a pure adsorption interaction takes place and no surface reactions occur.

The experiments conducted here provide new insights into the chemistry of oxidized polonium, which has remained largely unexplored due to the element's high radiotoxicity. Moreover, the results of this work offer valuable support for future chemical investigations of livermorium.

Author contributions

Katharina Hermainski: conceptualization, formal analysis, investigation, and writing – original draft; Alexander Yakushev: conceptualization, investigation, methodology, supervision, validation, and writing – review and editing; Dominik Dietzel: conceptualization, investigation, and writing – review and editing; Christoph Emanuel Düllmann: funding acquisition, investigation, supervision, validation, and writing – review and editing; Jochen Ballof, Pavol Mošat', Felix Sprunk and Maxim Saifulin: investigation and writing – review and editing; Pavel Bartl, Jan John, Mojmír Němec, Jon Petter Omtvedt, Jan Štursa and Václav Zach: investigation, resources, and writing – review and editing.

Conflicts of interest

There are no conflicts to declare.

Data availability

The raw data are available from the corresponding author upon reasonable request.

Data supporting this article have been included as part of the supplementary information (SI). Supplementary information is available. See DOI: https://doi.org/10.1039/d5cp04980f.

Acknowledgements

References

1 P. Thakur and A. L. Ward, *J. Radioanal. Nucl. Chem.*, 2020, **323**, 27–49.

2 B. R. R. Persson and E. Holm, *J. Environ. Radioact.*, 2011, **102**, 420–429.

3 C. D. Bowman, *Annu. Rev. Nucl. Part. Sci.*, 1998, **48**, 505–556.

4 E. A. Maugeri, J. Neuhausen, R. Eichler, R. Dressler, K. Rijpstra, S. Cottenier, D. Piguet, A. Vögele and D. Schumann, *Radiochim. Acta*, 2016, **104**, 757–767.

5 E. A. Maugeri, J. Neuhausen, R. Eichler, R. Dressler, K. Rijpstra, S. Cottenier, D. Piguet, A. Vögele and D. Schumann, *Radiochim. Acta*, 2016, **104**, 769–779.

6 E. A. Maugeri, J. Neuhausen, B. G. Prieto, A. Aerts, T. M. Mendonça, T. Stora and R. Eichler, *Radiochim. Acta*, 2018, **106**, 125–134.

7 P. Pyykkö, *Chem. Rev.*, 1988, **88**, 563–594.

8 A. Türler and V. Pershina, *Chem. Rev.*, 2013, **113**, 1237–1312.

9 A. Yakushev, J. Khuyagbaatar, Ch. E. Düllmann, M. Block, R. A. Cantemir, D. M. Cox, D. Dietzel, F. Giacoppo, Y. Hrabar, M. Iliaš, E. Jäger, J. Krier, D. Krupp, N. Kurz, L. Lens, S. Löchner, C. Mokry, P. Mošať, V. Pershina, S. Raeder, D. Rudolph, J. Runke, L. G. Sarmiento, B. Schausten, U. Scherer, P. Thörle-Pospiech, N. Trautmann, M. Wegrzecki and P. Wieczorek, *Front. Chem.*, 2024, **12**, 1474820.

10 V. Pershina, *Radiochim. Acta*, 2019, **107**, 833–863.

11 V. Pershina and M. Iliaš, *Mol. Phys.*, 2025, **123**, 2573831.

12 M. Schädel, *Radiochim. Acta*, 2012, **100**, 579–604.

13 A. F. Novgorodov, F. Rösch and N. A. Korolev, in *Handbook of Nuclear Chemistry - Instrumentation, separation techniques, environmental issues*, ed. A. Vertés, S. Nagy, Z. Klencsár, R. G. Lovas and F. Rösch, Springer, Dordrecht, 2nd edn, 2011, vol. 5, ch. 53, pp. 2429–2458.

14 I. Zvára, *Radiochim. Acta*, 1985, **38**, 95–101.

15 A. Yakushev, L. Lens, Ch. E. Düllmann, J. Khuyagbaatar, E. Jäger, J. Krier, J. Runke, H. M. Albers, M. Asai, M. Block, J. Despotopulos, A. Di Nitto, K. Eberhardt, U. Forsberg, P. Golubev, M. Götz, S. Götz, H. Haba, L. Harkness-Brennan, R.-D. Herzberg, F. P. Heßberger, D. Hinde, A. Hübner, D. Judson, B. Kindler, Y. Komori, J. Konki, J. V. Kratz, N. Kurz, M. Laatiaoui, S. Lahiri, B. Lommel, M. Maiti, A. K. Mistry, C. Mokry, K. J. Moody, Y. Nagame, J. P. Omtvedt, P. Papadakis, V. Pershina, D. Rudolph, L. G. Samiento, T. K. Sato, M. Schädel, P. Scharrer, B. Schausten, D. A. Shaughnessy, J. Steiner, P. Thörle-Pospiech, A. Toyoshima, N. Trautmann, K. Tsukada, J. Uusitalo, K.-O. Voss, A. Ward, M. Wegrzecki, N. Wiehl, E. Williams and V. Yakusheva, *Front. Chem.*, 2022, **10**, 976635.

16 J. Even, A. Yakushev, Ch. E. Düllmann, H. Haba, M. Asai, T. K. Sato, H. Brand, A. Di Nitto, R. Eichler, F. L. Fan, W. Hartmann, M. Huang, E. Jäger, D. Kaji, J. Kanaya, Y. Kaneya, J. Khuyagbaatar, B. Kindler, J. V. Kratz, J. Krier, Y. Kudou, N. Kurz, B. Lommel, S. Miyashita, K. Morimoto, K. Morita, M. Murakami, Y. Nagame, H. Nitsche, K. Ooe, Z. Qin, M. Schädel, J. Steiner, T. Sumita, M. Takeyama,

K. Tanaka, A. Toyoshima, K. Tsukada, A. Türler, I. Usoltsev, Y. Wakabayashi, Y. Wang, N. Wiehl and S. Yamaki, *Science*, 2014, **345**, 1491–1493.

17 R. Eichler, N. V. Aksenov, A. V. Belozerov, G. Bozhikov, V. I. Chepigin, S. N. Dmitriev, R. Dressler, H. W. Gäggeler, V. A. Gorshkov, F. Haenssler, M. G. Itkis, A. Laube, V. Y. Lebedev, O. N. Malyshev, Y. T. Oganessian, O. V. Petrushkin, D. Piguet, P. Rasmussen, S. V. Shishkin, A. V. Shutov, A. I. Svirikhin, E. E. Tereshatov, G. K. Vostokin, M. Wegrzecki and A. V. Yeremin, *Nature*, 2007, **447**, 72–75.

18 D. Dietzel, A. Yakushev and Ch. E. Düllmann, *J. Radioanal. Nucl. Chem.*, 2024, **333**, 3487–3496.

19 F. Weigel, *Angew. Chem., Int. Ed. Engl.*, 1959, **71**, 289–316.

20 K. W. Bagnall, in *Comprehensive inorganic chemistry*, ed. J. C. Bailar, H. J. Emeléus, Sir R. Nyholm and A. F. Trotman-Dickenson, Pergamon Press, Oxford, 1st edn, 1973, ch. 23–24, pp. 935–1008.

21 A. F. Holleman and N. Wiberg, *Lehrbuch der Anorganischen Chemie*, Walter de Gruyter, Berlin, 2007.

22 N. N. Greenwood and A. Earnshaw, in *Chemistry of the elements*, Elsevier, Amsterdam, 2nd edn, 1997, vol. 1, ch. 16, pp. 747–788.

23 K. W. Bagnall and R. W. M. D'Eye, *J. Chem. Soc.*, 1954, **1**, 4295–4299.

24 A. S. Abakumov, *Russ. Chem. Rev.*, 1982, **51**, 1091–1102.

25 K. W. Bagnall, *Radiochim. Acta*, 1983, **32**, 153–161.

26 R. H. Steinmeyer and C. J. Kershner, *J. Inorg. Nucl. Chem.*, 1971, **33**, 2847–2850.

27 H. Gäggeler, H. Dornhöfer, W. D. Schmidt-Ott, N. Greulich and B. Eichler, *Radiochim. Acta*, 1985, **38**, 103–106.

28 E. A. Maugeri, J. Neuhausen, R. Eichler, D. Piguet, T. M. Mendonça, T. Stora and D. Schumann, *J. Nucl. Mater.*, 2014, **450**, 292–298.

29 B. Eichler, *Kernenergie*, 1976, **19**, 307–311.

30 A. Vogt, H. W. Gäggeler and A. Türler, *Adsorption gas chromatography with 150-ms 216-Po*, Annual Report Paul Scherrer Institut, Villingen, 1996.

31 M. Gärtner, PhD thesis, University of Bern, 2001.

32 K. Hermainski, A. Yakushev, D. Dietzel, Ch. E. Düllmann, J. Ballof, P. Mošať, F. Sprunk, P. Bartl, J. John, J. Krier, M. Němec, J. P. Omtvedt and J. Štursa, *Phys. Chem. Chem. Phys.*, 2025, **27**, 21414–21423.

33 J. E. Shelby, *J. Non-Cryst. Solids*, 1994, **179**, 138–147.

34 A. P. Velmuzhov, M. V. Sukhanov, M. F. Churbanov, T. V. Kotereva, L. V. Shabarova and Y. P. Kirillov, *Inorg. Mater.*, 2018, **54**, 925–930.

35 I. Zvára, *The inorganic radiochemistry of heavy elements*, Springer, Luxembourg, 2008.

36 H. He and J. Yu, *J. Non-Cryst. Solids: X*, 2023, **18**, 100189.

37 D. Dietzel, A. Yakushev, Ch. E. Düllmann, K. Hermainski, J. Ballof, P. Bartl, R. Cantemir, J. John, J. Krier, P. Mošať, M. Němec, J. P. Omtvedt and J. Štursa, *J. Radioanal. Nucl. Chem.*, 2025, **334**, 6959–6972.

38 P. J. Eng, T. P. Trainor, G. E. Brown, G. A. Waychunas, M. Newville, S. R. Sutton and M. L. Rivers, *Science*, 2000, **288**, 1029–1033.

39 X. Yang, Z. Sun, D. Wang and W. Forsling, *J. Colloid Interface Sci.*, 2007, **308**, 395–404.

40 N. G. Petrik, P. L. Huestis, J. A. LaVerne, A. B. Aleksandrov, T. M. Orlando and G. A. Kimmel, *J. Phys. Chem. C*, 2018, **122**, 9540–9551.

41 D. Yang, M. Krasowska, R. Sedev and J. Ralston, *Phys. Chem. Chem. Phys.*, 2010, **12**, 13724–13729.

42 C. E. Nelson, J. W. Elam, M. A. Cameron, M. A. Tolbert and S. M. George, *Surf. Sci.*, 1998, **416**, 341–353.

43 K. C. Kang and D.-H. Yoon, *J. Eur. Ceram. Soc.*, 2022, **42**, 7508–7515.

44 K. C. Hass, W. F. Schneider, A. Curioni and W. Andreoni, *Science*, 1998, **282**, 265–268.

45 D. B. Mawhinney, J. A. Rossin, K. Gerhart and J. T. Yates, *Langmuir*, 2000, **16**, 2237–2241.

46 H. A. Al-Abadleh and V. H. Grassian, *Surf. Sci. Rep.*, 2003, **52**, 63–161.

47 P. Bartl, R. Běhal, T. Matlocha, M. Němec, P. Šváb, V. Zach, A. Bulíková, J. Štursa, J. P. Omtvedt and J. John, *Nucl. Instrum. Methods Phys. Res., Sect. A*, 2023, **1052**, 168280.

48 P. B. McGinnis and J. E. Shelby, *J. Non-Cryst. Solids*, 1994, **179**, 185–193.

49 R. Viswanathan, R. Balasubramanian, D. Darwin Albert Raj, M. Sai Baba and T. S. Lakshmi Narasimhan, *J. Alloys Compd.*, 2014, **603**, 75–85.

50 W. A. Dutton and W. C. Cooper, *Chem. Rev.*, 1966, **66**, 657–675.

51 E. A. Maugeri, J. Neuhausen, R. Eichler, D. Piguet and D. Schumann, *J. Nucl. Mater.*, 2014, **452**, 110–117.

52 B. Eichler, F. Zude, W. Fan, N. Trautmann and G. Herrmann, *Radiochim. Acta*, 1992, **56**, 133–140.

53 R. Eichler, B. Eichler, H. W. Gäggeler, D. T. Jost, R. Dressler and A. Türler, *Radiochim. Acta*, 1999, **87**, 151–160.

54 A. Vahle, S. Hübener, R. Dressler, B. Eichler and A. Türler, *Radiochim. Acta*, 1997, **78**, 53–57.

55 J. Goniakowski, F. Finocchi and C. Noguera, *Rep. Prog. Phys.*, 2008, **71**, 016501.

7628 | *Phys. Chem. Chem. Phys.*, 2026, **28**, 7617–7628

This journal is © the Owner Societies 2026